Axial form factor of the nucleon in the perturbative chiral quark model

K Khosonthongkee†‡, V E Lyubovitskij†, Th Gutsche†, Amand Faessler†, K Pumsa-ard†, S Cheedket‡ and Y Yan‡

† Institut für Theoretische Physik, Universität Tübingen, Auf der Morgenstelle 14, D-72076 Tübingen, Germany

‡ School of Physics, Suranaree University of Technology, Nakhon Ratchasima 30000, Thailand

E-mail: khoson@tphys.physik.uni-tuebingen.de, valeri.lyubovitskij@uni-tuebingen.de, thomas.gutsche@uni-tuebingen.de, amand.faessler@uni-tuebingen.de, pumsa@tphys.physik.uni-tuebingen.de, part@physics2.sut.ac.th, yupeng@ccs.sut.ac.th

Abstract.

We apply the perturbative chiral quark model (PCQM) at one loop to analyze the axial form factor of the nucleon. This chiral quark model is based on an effective Lagrangian, where baryons are described by relativistic valence quarks and a perturbative cloud of Goldstone bosons as dictated by chiral symmetry. We apply the formalism to obtain analytical expressions for the axial form factor of the nucleon, which is given in terms of fundamental parameters of low-energy pion-nucleon physics (weak pion decay constant, strong pion-nucleon form factor) and of only one model parameter (radius of the nucleonic three-quark core).

Submitted to: *J. Phys. G: Nucl. Phys.*

PACS numbers: 12.39.Ki, 13.30.Ce, 14.20.Dh

1. Introduction

The nucleon axial form factor is of fundamental significance to weak interaction properties and to the pion-nucleon interaction. Hence it provides one important test for theories that attempt to describe the structure of the nucleon. The current status of the experimental and theoretical understanding of the axial form factor of the nucleon is reviewed in [1, 2]. Based on the original development of chiral quark models with a perturbative treatment of the pion cloud [3]-[8], we recently extended the relativistic quark model suggested in [7, 8] to describe the low-energy properties of the nucleon [9]-[11]. In references [9]-[15] we developed the so-called perturbative chiral quark model (PCQM) in application to baryon properties such as: sigma-term physics, electromagnetic form factors of the baryon octet, πN scattering and electromagnetic corrections, strange nucleon form factors, electromagnetic nucleon-delta transition, etc. In the present work we follow up on the earlier investigations and employ the same model in order to study the axial form factor of the nucleon.

The PCQM is based on an effective chiral Lagrangian describing quarks as relativistic fermions moving in a self-consistent field (static potential) $V_{\rm eff}(r) = S(r) + \gamma^0 V(r)$ which is described by a sum of a scalar potential $S(r)$ providing confinement and the time component of a vector potential $\gamma^0 V(r)$. Obviously, other possible Lorenz structures (e.g., pseudoscalar or axial) are excluded by symmetry principles. It is known from lattice simulations that a scalar potential should be a linearly rising one and a vector potential thought to be responsible for short-range fluctuations of the gluon field configurations [16]. In our study we approximate $V_{\rm eff}(r)$ by a relativistic harmonic oscillator potential with a quadratic radial dependence [9]

$$S(r) = M_1 + c_1 r^2 \,, \quad V(r) = M_2 + c_2 r^2 \,. \tag{1}$$

The model potential defines unperturbed wave functions for the quarks, which are subsequently used to calculate baryon properties. This potential has no direct connection to the underlying physical picture and is thought to serve as an approximation of a realistic potential. The vector part of the potential is also a pure long-ranged potential and is not responsible for the short-range fluctuations of gluon fields. In general, we need a vector potential to distinguish between quark and antiquark solutions of the Dirac equation with an effective potential. Note, that this type of the potential was extensively used in chiral potential models [8],[17]-[22]. A positive feature of this potential is that most of the calculations can be done analytically. As was shown in Refs. [8],[17]-[22] and later on also checked in the PCQM [9]-[15], this effective potential gives a reasonable description of low-energy baryon properties and can be treated as a phenomenological approximation of the long-ranged potential dictated by QCD.

Baryons in the PCQM are described as bound states of valence quarks supplemented by a cloud of Goldstone bosons (π, K, η) as required by chiral symmetry. The chiral symmetry constraints will in general introduce a nonlinear meson-quark interaction, but when considering meson as small fluctuations we restrict the interaction Lagrangian up to the quadratic term in the meson fields. With the derived interaction Lagrangian

we do our perturbation theory in the expansion parameter $1/F$ (where F is the pion leptonic decay constant in the chiral limit). We also treat the mass term of the current quarks $(\hat{m}, m_s)$ as a perturbation. Dressing the baryonic three-quark core by a cloud of Goldstone mesons corresponds effectively to the inclusion of sea-quark contributions. All calculations are performed at one loop or at order of accuracy $O(1/F^2, \hat{m}, m_s)$.

To be consistent, we use the unified Dirac equation with a fixed static potential both for the ground and for the excited quark states. In the Appendix we give details of the solutions to the Dirac equation for any excited state. Inclusion of excited states should be handled consistently. First of all, one should guarantee conservation of local symmetries (like gauge invariance). Second, excited states should be restricted to energies smaller than the typical application scale $\Lambda \approx 1$ GeV of low-energy approaches. An alternative possibility to suppress the inclusion of higher-order excited states is to introduce a meson-quark vertex form factor [8, 19]. Solving the Dirac equation with a relativistic harmonic oscillator potential (1) one can show, that the energy shift between the first low-lying $1p$ excited states and the $1s$ ground state is about 200 MeV. The excited states ($1d$ and $2s$) lie about ~ 370 MeV above the ground state. The $2p$ and the $1f$ states are 530 MeV heavier when compared to the ground state. As soon as the typical energy of the ground-state quark is about 540 MeV‡one can restrict to the low-lying $1p$, $1d$ and $2s$ excited states with energies smaller than the typical scale $\Lambda = 1$ GeV. The requirement of convergence of physical observables when including excited states is physically not meaningful since it takes states with very large energies where the phenomenological low-energy approaches break down. One of us showed in Ref. [8] that the inclusion of excited states to the nucleon and Δ masses can be convergent when using a linearly rising confinement potential, e.g., the use of potential with a quadratic radial dependence leads to a nonsatisfactory convergence. However, this statement is sensitive to the quantity one is testing. On the other hand, our approach has some different features in comparison to previous ones (see, e.g., Ref. [8],[17]-[22]). In particular we perform a consistent renormalization procedure when we include meson cloud effects. It gives additional contributions to physical quantities which were not taken into account before. In Ref. [14] we demonstrated that excited quark states ($1p$, $1d$ and $2s$) can increase the contribution of loop diagrams but in comparison to the leading order (three-quark core) diagram this effect was of the order of 10%. This is why we were interested to study these effects for the example of the axial form factor. Again, we truncate the set of excited states to the $1p$, $1d$ and $2s$ state with energies which satisfy the condition $\mathcal{E} < \Lambda = 1$ GeV. We do not pretend that we have a more accurate estimate of the whole tower of excited states. The scheme we use is thought to take the excited states into account in an average fashion. We showed that the zeroth-order value of the axial nucleon charge is not changed much in the presence of meson cloud effects in consistency with chiral perturbation theory. As an extention of previous work, which is dominantly aimed to describe the low-energy static properties of baryons, we consider the model

‡ This value can be deduced from a calculation of octet and decouplet baryon spectrum. Similar estimates can be found in other chiral quark calculations.

prediction for the axial charge and for completeness also for the axial form factor. No further parameters are adjusted in the present work.

In the present paper we proceed as follows. First, we describe the basic features of our approach: the underlying effective Lagrangian, the unperturbed, that is valence quark, result for the nucleon description together with the choice of parameters and a brief overview of perturbation theory when including the meson fields. The full details of the renormalization technique can be found in reference [9]. In section III we concentrate on the detailed analysis of the nucleon axial form factor in our approach. We derive analytical expressions in terms of fundamental parameters of low-energy pion-nucleon physics (weak pion decay constant, strong pion-nucleon form factor) and of only one model parameter (radius of the three-quark core of the nucleon). Numerical results in comparison with data are presented to test the phenomenological implications of the model. Finally, section IV contains a summary of our major conclusions.

2. The perturbative chiral quark model

Following considerations lay out the basic notions of the perturbative chiral quark model (PCQM), a relativistic quark model suggested in [7, 8] and extended in [9]-[11] for the study of low-energy properties of baryons. In this model quarks move in an effective static field, represented by a scalar $S(r)$ and vector $V(r)$ component with $V_{\rm eff}(r) = S(r) + \gamma^0 V(r)$ and $r = |\boldsymbol{x}|$, providing phenomenological confinement. The interaction of quarks with Goldstone bosons is introduced on the basis of the nonlinear σ-model [23]. The PCQM is then defined by the effective, chirally invariant Lagrangian $\mathcal{L}_{\rm inv}$ [10, 11]

$$\mathcal{L}_{\rm inv}(x) = \bar\psi(x)\left\{ \mathrm{i}\,\partial\!\!\!/ - \gamma^0 V(r) - S(r)\left[\frac{U+U^\dagger}{2} + \gamma^5 \frac{U-U^\dagger}{2}\right]\right\}\psi(x) + \frac{F^2}{4}\,\mathrm{Tr}\left[\partial_\mu U\,\partial^\mu U^\dagger\right], \tag{2}$$

with an additional mass term for quarks and mesons

$$\mathcal{L}_{\chi SB}(x) = -\bar\psi(x)\mathcal{M}\psi(x) - \frac{B}{2}\,\mathrm{Tr}[\hat\Phi^2\mathcal{M}], \tag{3}$$

which explicitly breaks chiral symmetry. Here ψ is the quark field; $U = \mathrm{e}^{\mathrm{i}\hat\Phi/F}$ is the chiral field; $\hat\Phi$ is the matrix of pseudoscalar mesons (in the following we restrict to the $SU(2)$ flavor case, that is $\hat\Phi \to \hat\pi = \boldsymbol{\pi}\cdot\boldsymbol{\tau}$); $F = 88$ MeV is the pion decay constant in the chiral limit; $\mathcal{M} = \mathrm{diag}\{\hat m, \hat m\}$ is the mass matrix of current quarks (we restrict to the isospin symmetry limit with $m_u = m_d = \hat m = 7$ MeV) and $B = -\langle 0|\bar u u|0\rangle/F^2 = 1.4$ GeV is the quark condensate parameter. We rely on the standard picture of chiral symmetry breaking and for the mass of pions we use the leading term in their chiral expansion (i.e. linear in the current quark mass): $M_\pi^2 = 2\hat m B$.

With the unitary chiral rotation $\psi \to \exp\{-\mathrm{i}\gamma^5\hat\Phi/(2F)\}\psi$ [24]-[26] the Lagrangian (2) transforms into a Weinberg-type form $\mathcal{L}^W$ containing the axial-vector coupling

and the Weinberg-Tomozawa term [11]:

$$\begin{aligned}\mathcal{L}^W(x) &= \mathcal{L}_0(x) + \mathcal{L}_I^W(x) + o(\boldsymbol{\pi}^2), \\ \mathcal{L}_0(x) &= \bar{\psi}(x)\Big\{\mathrm{i}\,\partial\!\!\!/ - S(r) - \gamma^0 V(r)\Big\}\psi(x) - \frac{1}{2}\boldsymbol{\pi}(x)\left(\Box + M_\pi^2\right)\boldsymbol{\pi}(x), \\ \mathcal{L}_I^W(x) &= \frac{1}{2F}\partial_\mu\boldsymbol{\pi}(x)\bar{\psi}(x)\gamma^\mu\gamma^5\boldsymbol{\tau}\psi(x) - \frac{\varepsilon_{ijk}}{4F^2}\pi_i(x)\partial_\mu\pi_j(x)\bar{\psi}(x)\gamma^\mu\tau_k\psi(x),\end{aligned} \tag{4}$$

where $\mathcal{L}_I^W(x)$ is the $O(\boldsymbol{\pi}^2)$ strong interaction Lagrangian and $\Box = \partial^\mu\partial_\mu$.

In our calculation we do perturbation theory in the expansion parameter $1/F$ (where F is the pion leptonic decay constant in the chiral limit). We also treat the mass term of the current quarks as a perturbation. Dressing the baryonic three-quark core by a cloud of Goldstone mesons corresponds effectively to the inclusion of sea-quark contributions. All calculations are performed at one loop or at order of accuracy $O(1/F^2, \hat{m})$.

We expand the quark field ψ in the basis of potential eigenstates as

$$\psi(x) = \sum_\alpha b_\alpha u_\alpha(\boldsymbol{x})\mathrm{e}^{-\mathrm{i}\mathcal{E}_\alpha t} + \sum_\beta d_\beta^\dagger v_\beta(\boldsymbol{x})\mathrm{e}^{\mathrm{i}\mathcal{E}_\beta t}, \tag{5}$$

where the expansion coefficients b_α and $d_\beta^\dagger$ are the corresponding single quark annihilation and antiquark creation operators. The set of quark $\{u_\alpha\}$ and antiquark $\{v_\beta\}$ wave functions in orbits α and β are solutions of the static Dirac equation:

$$[-\mathrm{i}\gamma^0\boldsymbol{\gamma}\cdot\boldsymbol{\nabla} + \gamma^0 S(r) + V(r) - \mathcal{E}_\alpha]u_\alpha(\boldsymbol{x}) = 0, \tag{6}$$

where $\mathcal{E}_\alpha$ is the single quark energy.

The unperturbed nucleon state is conventionally set up by the product of spin-flavor and color quark wave functions, where the nonrelativistic single quark wave function is replaced by the relativistic solution $u_0(\boldsymbol{x})$ in the ground state.

For a given form of the effective potential $V_{\mathrm{eff}}(r)$ the Dirac equation in equation (6) can be solved numerically. Here, for the sake of simplicity, we use a variational Gaussian ansatz for the quark wave function given by the analytical form:

$$u_0(\boldsymbol{x}) \;=\; N_0\,\exp\left(-\frac{\boldsymbol{x}^{\,2}}{2R^2}\right)\,\begin{pmatrix}1\\ \mathrm{i}\rho\,\dfrac{\boldsymbol{\sigma}\,\boldsymbol{x}}{R}\end{pmatrix}\,\chi_s\,\chi_f\,\chi_c\,, \tag{7}$$

where $N_0 = \left[\pi^{3/2}R^3\left(1+\frac{3}{2}\rho^2\right)\right]^{-1/2}$ is a constant fixed by the normalization condition $\int \mathrm{d}^3\boldsymbol{x}\, u_0^\dagger(\boldsymbol{x})\, u_0(\boldsymbol{x}) \equiv 1$; χ_s, χ_f, χ_c are the spin, flavor and color quark wave functions, respectively. Our Gaussian ansatz contains two model parameters: the dimensional parameter R and the dimensionless parameter ρ. The parameter ρ can be related to the axial coupling constant $g_A^{(0)}$ calculated in zeroth-order (or three-quark core) approximation:

$$g_A^{(0)} = \frac{5}{3}\Big(1 - \frac{2\rho^2}{1+\frac{3}{2}\rho^2}\Big) = \frac{5}{3}\Big(\frac{1+2\gamma}{3}\Big), \tag{8}$$

where $\gamma = (1-\frac{3}{2}\rho^2)/(1+\frac{3}{2}\rho^2)$ is a relativistic reduction factor. In our calculations we use a value of $g_A^{(0)} = 1.25$ as obtained in the chiral limit of chiral perturbation theory [27]. The parameter R can be physically understood as the mean radius of the

three-quark core and is related to the charge radius of the proton in the leading-order (or zeroth-order) approximation as

$$\langle r_E^2 \rangle_{LO}^P = \int \mathrm{d}^3\boldsymbol{x} u_0^\dagger(\boldsymbol{x}) \boldsymbol{x}^2 u_0(\boldsymbol{x}) = \frac{3R^2}{2} \frac{1 + \frac{5}{2}\rho^2}{1 + \frac{3}{2}\rho^2}. \tag{9}$$

The parameter R was fixed as $R = 0.6$ fm in our previous study of electromagnetic properties of nucleon [9] which corresponds to $\langle r_E^2 \rangle_{LO}^P = 0.6$ fm^2.

The use of the Gaussian ansatz of equation (7) in its exact form restricts the scalar and the vector part of the potential to

$$S(r) = \frac{1 - 3\rho^2}{2\rho R} + \frac{\rho}{2R^3} r^2, \tag{10}$$

$$V(r) = \mathcal{E}_0 - \frac{1 + 3\rho^2}{2\rho R} + \frac{\rho}{2R^3} r^2. \tag{11}$$

The above expressions are introduced as a static mean field potential confinement in PCQM, hence covariance cannot be fulfilled. As a consequence matrix elements are frame dependent: both Galilei invariance of the zeroth order baryon wave functions and Lorentz boost effects, when considering finite momenta transfers, are neglected. Approximate techniques [28, 29] have been developed to account for these deficiencies in static potential models. However, these techniques do not always agree and lead to further ambiguities in model evaluations. Furthermore, existing Galilean projection techniques are known to lead to conflict with chiral symmetry constrains [10]. In the present manuscript we completely neglect the study of these additional model dependent effects. We focus on the role of meson loops, which, as shown in the content of cloudy bag model [29], are not plagued by these additional uncertainties.

According to the Gell-Mann and Low theorem we define the expectation value of an operator $\hat{\mathrm{O}}$ in the PCQM by

$$\langle \hat{\mathrm{O}} \rangle = {}^B\langle \phi_0 | \sum_{n=0}^{\infty} \frac{\mathrm{i}^n}{n!} \int \mathrm{d}^4x_1 \ldots \int \mathrm{d}^4x_n T[\mathcal{L}_I^W(x_1) \ldots \mathcal{L}_I^W(x_n) \hat{\mathrm{O}}] | \phi_0 \rangle_c^B. \tag{12}$$

The subscript c refers to contributions from connected graphs only and $\mathcal{L}_I^W(x)$ is the pion-quark interaction Lagrangian as already indicated in equation (4). The superscript B in equation (12) indicates that the matrix elements are projected on the respective baryon states. The projection of "one-body" diagrams on the nucleon state refers to

$$\chi_{f'}^\dagger \chi_{s'}^\dagger I^{f'f} J^{s's} \chi_f \chi_s \overset{Proj.}{\longrightarrow} \langle N | \sum_{i=1}^{3} (I\, J)^{(i)} | N \rangle, \tag{13}$$

where the single-particle matrix element of the operators I and J, acting in flavor and spin space, is replaced by the one embedded in the nucleon state. For "two-body" diagrams with two independent quark indices i and j the projection prescription reads as

$$\chi_{f'}^\dagger \chi_{s'}^\dagger I_1^{f'f} J_1^{s's} \chi_f \chi_s \otimes \chi_{k'}^\dagger \chi_{\sigma'}^\dagger I_2^{k'k} J_2^{\sigma'\sigma} \chi_k \chi_\sigma \overset{Proj.}{\longrightarrow} \langle N | \sum_{i \neq j}^{3} (I_1\, J_1)^{(i)} \otimes (I_2\, J_2)^{(j)} | N \rangle. \tag{14}$$

We evaluate equation (12) using Wick's theorem and the appropriate propagators. For the quark field we use a Feynman propagator for a fermion in a binding potential. The quark propagator $\mathrm{i}G_\psi(x,y)$ is given by

$$\mathrm{i}G_\psi(x,y) = \langle\phi_0|T\{\psi(x)\bar\psi(y)\}|\phi_0\rangle \to \sum_\alpha u_\alpha(\boldsymbol{x})\bar u_\alpha(\boldsymbol{y})\exp[-\mathrm{i}\mathcal{E}_\alpha(x_0-y_0)]\theta(x_0-y_0), \quad (15)$$

where we restrict to the quark states propagating forward in time. The explicit form of the excited quark wave functions are obtained analytically as given in Appendix. For the mesons we use the free Feynman propagator for a boson field with

$$\mathrm{i}\Delta_{ij}(x-y) = \langle 0|T\{\Phi_i(x)\Phi_j(y)\}|0\rangle = \delta_{ij}\int\frac{\mathrm{d}^4k}{(2\pi)^4\mathrm{i}}\frac{\exp[-\mathrm{i}k(x-y)]}{M_\Phi^2-k^2-\mathrm{i}\epsilon}. \quad (16)$$

To redefine our perturbation series up to a given order in terms of renormalized quantities a set of counterterms $\delta\mathcal{L}$ has to be introduced in the Lagrangian. Thereby, the counterterms play a dual role: (i) to maintain the proper definition of physical parameters, such as nucleon mass and, in particular, the nucleon charge, and (ii) to effectively reduce the number of Feynman diagrams to be evaluated. Here we follow the formalism set out in reference [9], but where in the present work intermediate excited quark states are included in the loop diagrams. In the following we attach the index "0" to the renormalization constants when we restrict to the contribution of the ground state quark propagator and the superscript "F" when excited quark states are included.

First we introduce the renormalized quark field $\psi^r(x)$. It can be expanded in a set of potential eigenstates which are solutions of the renormalized Dirac equation with the full renormalized quark mass of

$$\hat m_F^r = \hat m - \frac{3}{\gamma}\Big(\frac{1}{4\pi F}\Big)^2\sum_\alpha\int_0^\infty \mathrm{d}k\,k^2\,\frac{1}{\omega(k^2)(\omega(k^2)+\Delta\mathcal{E}_\alpha)} \times\Big[F_{I_\alpha}(k)F_{I_\alpha}^\dagger(k) - 2\omega(k^2)F_{I_\alpha}(k)F_{II_\alpha}^\dagger(k) + \omega^2(k^2)F_{II_\alpha}(k)F_{II_\alpha}^\dagger(k)\Big]. \quad (17)$$

The expression for the renormalized quark mass includes self-energy corrections of the pion cloud, where

$$F_{I_\alpha}(k) \equiv N_0N_\alpha k\Big[\int_0^\infty \mathrm{d}r\,r^2\,(g_0(r)g_\alpha(r)-f_0(r)f_\alpha(r))\int_\Omega \mathrm{d}\Omega\,\mathrm{e}^{\mathrm{i}kr\cos\theta}\,C_\alpha\,Y_{l_\alpha 0}(\theta,\phi) -2\,\mathrm{i}\frac{\partial}{\partial k}\int_0^\infty \mathrm{d}r\,r\,(f_0(r)f_\alpha(r))\int_\Omega \mathrm{d}\Omega\,\cos\theta\,\mathrm{e}^{\mathrm{i}kr\cos\theta}\,C_\alpha\,Y_{l_\alpha 0}(\theta,\phi)\Big], \quad (18)$$

$$F_{II_\alpha}(k) \equiv N_0N_\alpha\frac{\partial}{\partial k}\int_0^\infty \mathrm{d}r\,r\,(g_0(r)f_\alpha(r)-f_0(r)g_\alpha(r))\int_\Omega \mathrm{d}\Omega\,\mathrm{e}^{\mathrm{i}kr\cos\theta}\,C_\alpha\,Y_{l_\alpha 0}(\theta,\phi), \quad (19)$$

with the pion energy $\omega(k^2)=\sqrt{M_\pi^2+k^2}$; $k=|\boldsymbol{k}|$ is the pion momentum and $\Delta\mathcal{E}_\alpha = \mathcal{E}_\alpha-\mathcal{E}_0$ is the excess of the energy of the quark in state α with respect to the ground state. The label $\alpha=(nl_\alpha jm)$ characterizes the quark state (principal quantum number n, non-relativistic orbital angular momentum l_α, total angular momentum and projection j,m). For the Clebsch-Gordan coefficients we use the notation $C_\alpha \equiv \langle l_\alpha 0\frac{1}{2}\frac{1}{2}|j\frac{1}{2}\rangle$ and $Y_{l_\alpha 0}(\theta,\phi)$ is the usual spherical harmonic. The explicit form of the radial wave functions $g_\alpha(r)$

and $f_\alpha(r)$, of the normalization constants (N_α) and of the energy difference ($\Delta\mathcal{E}_\alpha$) are given in Appendix.

When restricting the quark propagator to the ground state the expression above for the renormalized quark mass reduces to

$$\hat{m}_0^r = \hat{m} - \frac{27}{400\gamma}\left(\frac{g_A^{(0)}}{\pi F}\right)^2 \int_0^\infty \mathrm{d}k\, k^4\, \frac{F_{\pi NN}^2(k^2)}{\omega^2(k^2)}, \tag{20}$$

where $F_{\pi NN}(k^2)$ is the πNN form factor normalized to unity at zero recoil ($k^2 = 0$):

$$F_{\pi NN}(k^2) = \exp\left(-\frac{k^2R^2}{4}\right)\left[1 + \frac{k^2R^2}{8}\left(1 - \frac{5}{3g_A^{(0)}}\right)\right]. \tag{21}$$

In a second step we renormalize the effective Lagrangian including a set of counterterms. The renormalized interaction Lagrangian $\mathcal{L}_{I;r}^W = \mathcal{L}_{I;r}^{W;str} + \mathcal{L}_{I;r}^{W;em}$ contains a part due to the strong interaction,

$$\mathcal{L}_{I;r}^{W;str} = \mathcal{L}_I^{W;str} + \delta\mathcal{L}^{W;str}, \tag{22}$$

and a piece due to the electromagnetic interaction,

$$\mathcal{L}_{I;r}^{W;em} = \mathcal{L}_I^{W;em} + \delta\mathcal{L}^{W;em}. \tag{23}$$

The strong interaction term $\mathcal{L}_I^{W;str}$ is given by

$$\mathcal{L}_I^{W;str}(x) = \frac{1}{2F}\partial_\mu\boldsymbol{\pi}(x)\bar{\psi}^r(x)\gamma^\mu\gamma^5\boldsymbol{\tau}\psi^r(x) - \frac{\varepsilon_{ijk}}{4F^2}\pi_i(x)\partial_\mu\pi_j(x)\bar{\psi}^r(x)\gamma^\mu\tau_k\psi^r(x). \tag{24}$$

The interaction of pions and quarks with the electromagnetic field is described by [11]

$$\begin{aligned}\mathcal{L}_I^{W;em}(x) = &-eA_\mu^{em}\bar{\psi}^r(x)Q\gamma^\mu\psi^r(x) + \frac{e}{4F^2}A_\mu^{em}(x)\bar{\psi}^r(x)\gamma^\mu\left[\boldsymbol{\pi}^2(x)\tau_3 - \boldsymbol{\pi}(x)\boldsymbol{\tau}\pi^0(x)\right]\psi^r(x)\\ &-eA_\mu^{em}(x)\varepsilon_{3ij}\left[\pi_i(x)\partial^\mu\pi_j(x) - \frac{\pi_j(x)}{2F}\bar{\psi}^r(x)\gamma^\mu\gamma^5\tau_i\psi^r(x)\right],\end{aligned} \tag{25}$$

which is generated by minimal substitution with

$$\partial_\mu\psi^r \to D_\mu\psi^r = \partial_\mu\psi^r + \mathrm{i}eQA_\mu^{em}\psi^r, \qquad \partial_\mu\pi_i \to D_\mu\pi_i = \partial_\mu\pi_i + e\varepsilon_{3ij}A_\mu^{em}\pi_j, \tag{26}$$

where Q is the quark charge matrix. The set of counterterms, denoted by $\delta\mathcal{L}^{W;str}$ and $\delta\mathcal{L}^{W;em}$ are explained and given in reference [9].

Now we consider the nucleon charge and prove that the properly introduced counterterms guarantee charge conservation. Using Noether's theorem we first derive from the renormalized Lagrangian the electromagnetic current operator:

$$j_r^\mu = j_{\psi^r}^\mu + j_\pi^\mu + j_{\psi^r\pi}^\mu + \delta j_{\psi^r}^\mu. \tag{27}$$

It contains the quark component ($j_{\psi^r}^\mu$), the charged pion component (j_π^μ), the quark-pion component ($j_{\psi^r\pi}^\mu$) and the contribution of the counterterm ($\delta j_{\psi^r}^\mu$):

$$\begin{aligned} j_{\psi^r}^\mu &= \bar{\psi}^r\gamma^\mu Q\psi^r = \frac{1}{3}\left(2\bar{u}^r\gamma^\mu u^r - \bar{d}^r\gamma^\mu d^r\right),\\ j_\pi^\mu &= \varepsilon_{3ij}\,\pi_i\partial^\mu\pi_j \;=\; \pi^-\mathrm{i}\partial^\mu\pi^+ - \pi^+\mathrm{i}\partial^\mu\pi^-,\\ j_{\psi^r\pi}^\mu &= -\frac{1}{4F^2}\bar{\psi}^r\gamma^\mu\left(\boldsymbol{\pi}^2\tau_3 - \boldsymbol{\pi}\,\boldsymbol{\tau}\pi^0\right)\psi^r - \varepsilon_{3ij}\frac{\pi_j}{2F}\bar{\psi}^r\gamma^\mu\gamma^5\tau_i\psi^r,\\ \delta j_{\psi^r}^\mu &= \bar{\psi}^r(\hat{Z}-1)\gamma^\mu Q\psi^r \end{aligned} \tag{28}$$

Here, $\hat{Z}$ is the renormalization constant determined by the nucleon charge conservation condition [9]. In the one-loop approximation following diagrams contribute to the nucleon charge [Figs.1a-1f]: the three-quark diagram [Fig.1a] with an insertion of the quark current $j^{\mu}_{\psi^r}$, the three-quark diagram [Fig.1b] with the counterterm $\delta j^{\mu}_{\psi^r}$ (three-quark counterterm diagram), the self-energy [Figs.1c and 1d], the vertex correction diagram [Fig.1e] with the quark current $j^{\mu}_{\psi^r}$, and finally the meson-cloud diagram [Fig.1f] generated by the pion current j^{μ}_{π}.

The analytical expression for the full renormalization constant, $\hat{Z}^F$ is

$$\hat{Z}^F = 1 - \frac{3}{(4\pi F)^2}\sum_{\alpha}\int_0^{\infty} \mathrm{d}k\, k^2\, \frac{1}{\omega(k^2)(\omega(k^2)+\Delta\mathcal{E}_{\alpha})^2} \times \Big[F_{I_\alpha}(k)F^{\dagger}_{I_\alpha}(k) - 2\,\omega(k^2)F_{I_\alpha}(k)F^{\dagger}_{II_\alpha}(k) + \omega^2(k^2)F_{II_\alpha}(k)F^{\dagger}_{II_\alpha}(k)\Big]. \quad (29)$$

When restricting intermediate quark states to the ground state equation (29) yields the result

$$\hat{Z}^0 = 1 - \frac{27}{400}\left(\frac{g_A^{(0)}}{\pi F}\right)^2 \int_0^{\infty} \mathrm{d}k\, k^4\, \frac{F^2_{\pi NN}(k^2)}{\omega^3(k^2)}. \quad (30)$$

We obtain a value of $\hat{Z}^0 = 0.9$ [9] for our set of parameters. Inclusion of the excited quark states changes the value of the renormalization constant to a value of $\hat{Z}^F = 0.7$.

3. The axial form factor of nucleon

For the present purposes we have to construct the partially conserved axial-vector current A^{μ}_i:

$$A^{\mu}_i = F\partial^{\mu}\pi_i + \bar{\psi}^r\gamma^{\mu}\gamma^5\frac{\tau_i}{2}\psi^r - \frac{\varepsilon_{ijk}}{2F}\bar{\psi}^r\gamma^{\mu}\tau_j\psi^r\pi_k + \frac{1}{4F^2}\,\bar{\psi}^r\gamma^{\mu}\gamma^5\left(\boldsymbol{\pi}\,\boldsymbol{\tau}\,\pi_i - \boldsymbol{\pi}^2\,\tau_i\right)\psi^r \quad (31)$$
$$+\bar{\psi}^r(\hat{Z}-1)\gamma^{\mu}\gamma^5\frac{\tau_i}{2}\psi^r + o(\boldsymbol{\pi}^2)\,.$$

The axial form factor $G_A(Q^2)$ of the nucleon is defined by the matrix element of the $i=3$ isospin component and the spatial part of the axial vector current evaluated for nucleon states. In the Breit frame $G_A(Q^2)$ is set up as [18]:

$$\left\langle N_{s'}\left(\frac{\boldsymbol{q}}{2}\right)\Big|\int \mathrm{d}^3\boldsymbol{x}\,\mathrm{e}^{\mathrm{i}\boldsymbol{q}\,\boldsymbol{x}}\boldsymbol{A}_3(x)\Big|N_s\left(-\frac{\boldsymbol{q}}{2}\right)\right\rangle = \chi^{\dagger}_{N_{s'}}\boldsymbol{\sigma}_N\frac{\tau^3_N}{2}\chi_{N_s}G_A(Q^2), \quad (32)$$

with $Q^2 = -q^2$. Here, χ_{N_s} and $\chi_{N_{s'}}$ are the nucleon spin wave functions in the initial and final states; $\boldsymbol{\sigma}_N$ is the nucleon spin matrix and τ^3_N is the third component of the isospin matrix of the nucleon. At zero recoil ($Q^2=0$) the axial form factor satisfies the condition $G_A(0) = g_A$, where g_A is axial charge of the nucleon.

In the PCQM the axial form factor of the nucleon up to one loop corrections is initially given by

$$\chi^{\dagger}_{N_{s'}}\boldsymbol{\sigma}_N\frac{\tau^3_N}{2}\chi_{N_s}G_A(Q^2) = {}^N\langle\phi_0|\sum_{n=0}^{2}\frac{\mathrm{i}^n}{n!}\int \delta(t)\,\mathrm{d}^4x\,\mathrm{d}^4x_1\,\ldots\,\mathrm{d}^4x_n\,\mathrm{e}^{-\mathrm{i}qx} \times T[\mathcal{L}^{W;str}_I(x_1)\,\ldots\,\mathcal{L}^{W;str}_I(x_n)\,\boldsymbol{A}_3(x)]\,|\phi_0\rangle^N_c, \quad (33)$$

with the interaction term

$$\mathcal{L}_I^{W;str}(x) = \frac{1}{2F}\partial_\mu \boldsymbol{\pi}(x)\bar{\psi}^r(x)\gamma^\mu\gamma^5\boldsymbol{\tau}\psi^r(x) - \frac{\varepsilon_{ijk}}{4F^2}\pi_i(x)\partial_\mu\pi_j(x)\bar{\psi}^r(x)\gamma^\mu\tau_k\psi^r(x), \tag{34}$$

where the superscript r refers to renormalized quantities. For the final calculation we include a set of excited states up to $2\hbar\omega$ in the quark propagator: the first p-states ($1p_{1/2}$ and $1p_{3/2}$ in the non-relativistic spectroscopic notation) and the second excited states ($1d_{3/2}$, $1d_{5/2}$ and $2s_{1/2}$). In other words we include the excited states whose energies satisfy to the restriction $\mathcal{E} < \Lambda = 1$ GeV (see discussion in the Sect.1). The diagrams to be evaluated are shown in Fig.2.

Next, we present the analytical expressions for the axial form factor of the nucleon obtained in the PCQM. We start with the simplest case, where the quark propagator is restricted to the ground state contribution. The axial form factor of the nucleon is a sum of terms arising from different diagrams: the three-quarks diagram [Fig.2a], the counterterm [Fig.2b], the self-energy diagrams [Figs.2c and 2d], the exchange diagram [Fig.2e] and the vertex-correction diagram [Fig.2f]. Other possible diagrams at one loop are compensated by the counterterm. The corresponding analytical expressions for the relevant diagrams are given in the following.

(a) For the three-quark diagram ($3q$) [Fig.2a] we obtain:

$$G_A(Q^2)\Big|_{3q} = G_A(Q^2)\Big|_{3q}^{LO} + G_A(Q^2)\Big|_{3q}^{NLO}, \tag{35}$$

where $G_A(Q^2)|_{3q}^{LO}$ is the leading-order term (LO) evaluated with the unperturbed quark wave function (w.f.) $u_0(\boldsymbol{x})$; $G_A(Q^2)|_{3q}^{NLO}$ is a correction due to the renormalization of the quark w.f. $u_0(\boldsymbol{x}) \to u_0^r(\boldsymbol{x};\hat{m}^r)$ which is referred to as next-to-leading order (NLO):

$$G_A(Q^2)\Big|_{3q}^{LO} = g_A^{(0)} F_{\pi NN}(Q^2) \tag{36}$$

$$G_A(Q^2)\Big|_{3q}^{NLO} = \frac{3}{2}\,\hat{m}_0^r \frac{\rho\, R}{\left(1+\frac{3}{2}\rho^2\right)^2}\left\{\left(1+\frac{9}{2}\rho^2\right) G_A(Q^2)\Big|_{3q}^{LO} - \frac{5}{72}\Big[12\left(2-3\rho^2\right) - 4\left(1+5\rho^2\right)Q^2R^2 + \rho^2Q^4R^4\Big]\exp\left(-\frac{Q^2R^2}{4}\right)\right\}. \tag{37}$$

The modified quark w.f. $u_0^r(\boldsymbol{x};\hat{m}^r)$ is given by [9]

$$u_0^r(\boldsymbol{x};\hat{m}^r) = u_0(\boldsymbol{x}) + \delta u_0^r(\boldsymbol{x};\hat{m}^r), \tag{38}$$

where

$$\delta u_0^r(\boldsymbol{x};\hat{m}^r) = \frac{\hat{m}^r}{2}\frac{\rho R}{1+\frac{3}{2}\rho^2}\left(\frac{\frac{1}{2}+\frac{21}{4}\rho^2}{1+\frac{3}{2}\rho^2} - \frac{\boldsymbol{x}^2}{R^2} + \gamma^0\right) u_0(\boldsymbol{x}). \tag{39}$$

(b) The three-quark counterterm (CT) [Fig.2b] results in the expression:

$$G_A(Q^2)\Big|_{CT} \equiv (\hat{Z}^0 - 1) G_A(Q^2)\Big|_{3q}^{LO}. \tag{40}$$

(c) The self-energy diagram I (SE;I) [Fig.2c] yields:

$$G_A(Q^2)\Big|_{SE;I} = 8\, g_A^{(0)}\, \frac{\rho\, R}{(2+3\rho^2)}\left(\frac{1}{2\pi F}\right)^2 \int_0^\infty \mathrm{d}k\, k^4 \frac{F_{\pi NN}(k^2)}{\omega^2(k^2)}\, \mathcal{D}(k,Q^2), \tag{41}$$

where

$$\mathcal{D}(k,Q^2) \equiv \exp\left(-\frac{(k+\sqrt{Q^2})^2R^2}{4}\right)\left(\frac{1}{k^2Q^2R^4}\right)^{3/2} \times\left[2+k\sqrt{Q^2}R^2+\exp\left(k\sqrt{Q^2}R^2\right)\left(-2+k\sqrt{Q^2}R^2\right)\right]. \quad (42)$$

(d) For the self-energy diagram II (SE;II) [Fig.2d] we also obtain:

$$G_A(Q^2)\Big|_{SE;II} = G_A(Q^2)\Big|_{SE;I}. \quad (43)$$

(e) For the exchange diagram (EX) [Fig.2e] we get:

$$G_A(Q^2)\Big|_{EX} = \frac{96}{5}\, g_A^{(0)}\, \frac{\rho\, R}{(2+3\rho^2)}\left(\frac{1}{2\pi F}\right)^2 \int_0^\infty \mathrm{d}k\, k^4 \frac{F_{\pi NN}(k^2)}{\omega^2(k^2)}\, \mathcal{D}(k,Q^2). \quad (44)$$

(f) The vertex-correction diagram (VC) [Fig.2f] gives the contribution:

$$G_A(Q^2)\Big|_{VC} = \frac{3}{100}\left(g_A^{(0)}\right)^3\left(\frac{1}{2\pi F}\right)^2 F_{\pi NN}(Q^2)\int_0^\infty \mathrm{d}k\, k^4\, \frac{F^2_{\pi NN}(k^2)}{\omega^3(k^2)}. \quad (45)$$

In the next step we extend the formalism by also including excited states in the quark propagator. The leading-order expression of the three-quark diagram and the exchange term remain the same. In turn the following contributions must be extended.

(a) In the three-quark NLO expression the appropriate renormalized mass has to be inserted with

$$G_A(Q^2)\Big|_{3q}^{NLO} = \frac{3}{2}\,\hat{m}_F^r \frac{\rho\, R}{\left(1+\frac{3}{2}\rho^2\right)^2}\left\{\left(1+\frac{9}{2}\rho^2\right) G_A(Q^2)\Big|_{3q}^{LO} -\frac{5}{72}\left[12\left(2-3\rho^2\right)-4\left(1+5\rho^2\right)Q^2R^2+\rho^2Q^4R^4\right]\exp\left(-\frac{Q^2R^2}{4}\right)\right\}. \quad (46)$$

(b) For the three-quark counterterm (CT) the renormalization constant has to be replaced accordingly

$$G_A(Q^2)\Big|_{CT} = (\hat{Z}^F-1)G_A(Q^2)\Big|_{3q}^{LO}. \quad (47)$$

(c) For the self-energy diagram I (SE;I) we obtain the full expression

$$G_A(Q^2)\Big|_{SE;I} = \frac{10}{3}\left(\frac{1}{4\pi F}\right)^2 \sum_\alpha \int_0^\infty \mathrm{d}k\, k^2\, \frac{\omega(k^2)F_{II_\alpha}(k)-F_{I_\alpha}(k)}{\omega(k^2)(\omega(k^2)+\Delta\mathcal{E}_\alpha)} \times\int_{-1}^1 \mathrm{d}x\, \frac{2k(1-x^2)F_{III_\alpha}(k_-)+\left(\sqrt{Q^2}x+(1-2x^2)k\right)F_{IV_\alpha}(k_-)}{\sqrt{k_-^2}}, \quad (48)$$

where

$$F_{III_\alpha}(k_-) \equiv N_0N_\alpha\frac{\partial}{\partial k_-}\int_0^\infty \mathrm{d}r\, r\,(g_0(r)f_\alpha(r))\int_\Omega \mathrm{d}\Omega\, \mathrm{e}^{\mathrm{i}k_-\, r\,\cos\theta}C_\alpha Y_{l_\alpha 0}(\theta,\phi),$$

$$F_{IV_\alpha}(k_-) \equiv N_0N_\alpha\frac{\partial}{\partial k_-}\int_0^\infty \mathrm{d}r\, r\,(f_0(r)g_\alpha(r)-g_0(r)f_\alpha(r)) \times\int_\Omega \mathrm{d}\Omega\, \mathrm{e}^{\mathrm{i}k_-\, r\,\cos\theta}C_\alpha Y_{l_\alpha 0}(\theta,\phi),$$

$$k_\pm^2 \equiv k^2+Q^2\pm 2k\sqrt{Q^2}x. \quad (49)$$

(d) For the self-energy diagram II (SE;II) we get

$$G_A(Q^2)\Big|_{SE;II} = \frac{10}{3}\left(\frac{1}{4\pi F}\right)^2 \sum_\alpha \int_0^\infty \mathrm{d}k\, k^2\, \frac{\omega(k^2)F^\dagger_{II_\alpha}(k) - F^\dagger_{I_\alpha}(k)}{\omega(k^2)(\omega(k^2)+\Delta\mathcal{E}_\alpha)} \times \int_{-1}^1 \mathrm{d}x\, \frac{2k(1-x^2)F_{V_\alpha}(k_+) - (\sqrt{Q^2}x+k)F_{IV_\alpha}(k_+)}{\sqrt{k_+^2}}, \tag{50}$$

where

$$F_{V_\alpha}(k_+) \equiv N_0 N_\alpha \frac{\partial}{\partial k_+}\int_0^\infty \mathrm{d}r\, r\,(f_0(r)g_\alpha(r)) \int_\Omega \mathrm{d}\Omega \mathrm{e}^{\mathrm{i}k_+\, r\, \cos\theta} C_\alpha Y_{l_\alpha 0}(\theta,\phi). \tag{51}$$

(e) For the vertex-correction diagram (VC) inclusion of excited states results in

$$G_A(Q^2)\Big|_{VC} = \sum_{\alpha\,\beta}\frac{5}{9}\frac{\mathcal{F}_{\alpha,\beta}(Q^2)}{(4\pi F)^2}\int_0^\infty \mathrm{d}k\, k^2\, \left[\frac{1}{\omega(k^2)(\omega(k^2)+\Delta\mathcal{E}_\alpha)\,(\omega(k^2)+\Delta\mathcal{E}_\beta)}\right] \times\Big[\omega^2(k^2)\left(F_{II_\alpha}(k)F^\dagger_{II_\beta}(k)\right) - \omega(k^2)\left(F_{II_\alpha}(k)F^\dagger_{I_\beta}(k) + F_{I_\alpha}(k)F^\dagger_{II_\beta}(k)\right) + \left(F_{I_\alpha}(k)F^\dagger_{I_\beta}(k)\right)\Big], \tag{52}$$

where

$$\mathcal{F}_{\alpha,\beta}(Q^2) \equiv N_\alpha N_\beta \int_0^\infty \mathrm{d}r\, r^2\Big(\mathcal{A}_{\alpha,\beta}(r) + 2\mathcal{B}_{\alpha,\beta}(r)\Big), \tag{53}$$

$$\mathcal{A}_{\alpha,\beta}(r) \equiv (g_\alpha(r)g_\beta(r) - f_\alpha(r)f_\beta(r)) \int_\Omega \mathrm{d}\Omega\, \exp\left(\mathrm{i}\sqrt{Q^2}r\cos\theta\right)\, \mathcal{C}_{\alpha\beta;1}(\theta,\phi), \tag{54}$$

$$\mathcal{B}_{\alpha,\beta}(r) \equiv f_\alpha(r)f_\beta(r)\int_\Omega \mathrm{d}\Omega\, \exp\left(\mathrm{i}\sqrt{Q^2}r\cos\theta\right) \times\Big[\cos^2\theta\, \mathcal{C}_{\alpha\beta;1}(\theta,\phi) + \sin\theta\,\cos\theta\, \mathcal{C}_{\alpha\beta;2}(\theta,\phi)\Big], \tag{55}$$

$$\mathcal{C}_{\alpha\beta;1}(\theta,\phi) \equiv C_\alpha C_\beta Y_{l_\alpha 0}(\theta,\phi)Y_{l_\beta 0}(\theta,\phi) - D_\alpha D_\beta Y^*_{l_\alpha 1}(\theta,\phi)Y_{l_\beta 1}(\theta,\phi), \tag{56}$$

$$\mathcal{C}_{\alpha\beta;2}(\theta,\phi) \equiv C_\alpha D_\beta Y_{l_\alpha 0}(\theta,\phi)Y_{l_\beta 1}(\theta,\phi)\mathrm{e}^{-\mathrm{i}\phi} + D_\alpha C_\beta Y^*_{l_\alpha 1}(\theta,\phi)Y_{l_\beta 0}(\theta,\phi)\mathrm{e}^{\mathrm{i}\phi}, \tag{57}$$

where $D_\alpha = \langle l_\alpha 1\frac{1}{2}\,-\frac{1}{2}|j\frac{1}{2}\rangle$, l_α and l_β are the orbital quantum numbers of the intermediate states α and β, respectively.

The Q^2-dependence (up to $0.4\,\mathrm{GeV}^2$) of the axial form factor of the nucleon are shown in Figs.3, 4 and 5, the description of each figure is given below. Due to the lack of covariance, the form factor can be expected to be reasonable up to $Q^2 < \boldsymbol{p}^2 = 0.4\,\mathrm{GeV}^2$, where $\boldsymbol{p}$ is the typical three-momentum transfer which defines the region where relativistic effect $\leq$ 10% or where the following inequality $\boldsymbol{p}^2/\,(4m_N^2) < 0.1$ is fulfilled.

The first result for the Q^2-dependence of the axial form factor $G_A(Q^2)$ of the nucleon is indicated in Fig.3. The numerical values are obtained, when truncating the quark propagator to the ground state or equivalently to the intermediate nucleon and delta baryon states in loop diagrams. Thereby, we also give the individual contributions of the different diagrams of Fig.2, which add up coherently. The leading order three-quark diagram dominates the result for the axial form factor, whereas pion cloud corrections

add about 20% of the total result. Here, both the exchange and self-energy terms give the largest, positive contribution.

In a next step we include the intermediate excited quark states with quantum numbers $1p_{1/2}, 1p_{3/2}, 1d_{3/2}, 1d_{5/2}$ and $2s_{1/2}$ in the propagator. The resulting effect on $G_A(Q^2)$ is given in Fig.4. We explicitly indicate the additional terms, which are solely due to the contribution of these excited states. The previous result, where the quark propagator is restricted to the ground state, is contained in the curve denoted by Total(GS). The inclusion of the intermediate excited states tends to induce a cancellation of the original pion cloud corrections generated for the case of the ground state quark propagator, thereby regaining approximately the tree level result. In Fig.5 we give for completeness the full result for $G_A(Q^2)$ including excited states in comparison with experimental data and with the dipole fit using an axial mass of $M_A = 1.069$ GeV and normalized to $G_A(0) = 1.267$ at zero recoil. The model clearly underestimates the finite Q^2-behavior, but it should be noted that a similar effect occurs in the discussion of the electromagnetic form factors of the nucleon [9]. The stiffness of the form factors can be traced to the Gaussian ansatz of the single quark wave functions and can also be improved when in addition resorting to a fully covariant description of the valence quark content of the nucleon [30]. Hence the applicability of the PCQM is mostly for static quantities and low Q^2 observables of baryons.

For the comparison with the data near $Q^2 = 0$ we first turn to the results for the axial charge, g_A. In Table 1 we list the numerical values for the complete set of Feynman diagrams (Fig.2), again indicating separately the contributions of ground and excited states in the quark propagator.

The prediction for the axial charge including loop corrections are relevant for several reasons: 1) the tree level result for g_A was previously adjusted to fix one (ρ) of the parameters. Since loop corrections essentially do not change this results, the previous model predictions remain meaningful; 2) the predicted small loop corrections to g_A are consistent with similar results in chiral perturbation theory; 3) the generic role of excited states in loop diagrams are rather relevant in understanding the nucleon properties. This role was already exemplified in the case of $N - \Delta$ transition [14] and sigma-terms [15] and again is demonstrated in the case of g_A.

For low-momentum transfers, that is $Q^2 \leq 1$ GeV^2, the axial form factor can be represented by a dipole fit

$$G_A(Q^2) = \frac{G_A(0)}{(1 + \frac{Q^2}{M_A^2})^2}, \tag{58}$$

in terms of one adjustable parameter M_A, the axial mass (or sometimes dipole mass). Therefore, the axial radius can be expressed in terms of the axial mass with:

$$\langle r_A^2 \rangle = -6 \frac{1}{G_A(0)} \frac{dG_A(Q^2)}{dQ^2}\Big|_{Q^2=0} = \frac{12}{M_A^2}. \tag{59}$$

A comparison of the experimentally deduced values for the axial mass and the axial radius with our model results is given in Table 2.

4. Summary and Conclusions

In summary, we have evaluated the axial form factor of the nucleon and, more important, its low Q^2 limits, such as the axial charge and the axial radius using a perturbative chiral quark model as based on an effective chiral Lagrangian. Since the PCQM is a static model, Lorentz covariance cannot be fulfilled. Approximate techniques to account for Galilei invariance and Lorentz boost effects were shown to change the tree level results by about 10%. Higher order, that is loop contributions, are less sensitive to these correction. The derived quantities contain, in consistency with previous works, only one model parameter R, which is related to the radius of the three-quark core, and are otherwise expressed in terms of fundamental parameters of low energy hadron physics: weak pion decay constant, and set of QCD parameters. In addition, another parameter (ρ of equation (6)), which is related to the amplitude of the small component of the single quark wave function, was originally set up to reproduce the value for the axial charge in the chiral limit with $g_A^{(0)} = 1.25$ [27]. Predictions are given for the fixed values of model parameters ρ and R in consistency with previous investigations. In particular, our result for the axial charge, $g_A = 1.19$, is in reasonable agreement with the central value of data: $g_A = 1.267 \pm 0.003$. Thereby, contributions of excited quark states in loop diagrams play a considerable role in order to generate a small correction to the tree level result, which is required to account for the data point. This result, obtained in the context of the PCQM, is rather encouraging. Minor pion cloud corrections to the tree level result of g_A justify in turn the appropriate choice for ρ or for $g_A^{(0)}$ used in previous works. Also, recent calculations of the axial charge up to order p^4 in chiral perturbation theory [31, 32] imply rather large p^3 corrections leading to rather large uncertainties when going to the next order in the chiral expansion. Our model result can naturally explain the small correction to the one obtained in the chiral limit, but only when going beyond nucleon and delta states in the loop diagrams.

Acknowledgments

This work was supported by the Deutsche Forschungsgemeinschaft (DFG Nos.FA67/25-3, GRK 683). K. K., S. C. and Y. Y. acknowledge the support of Thailand Research Fund (TRF, Grant No.RGJ PHD/00187/2541, PHD/00165/2541) and the Deutscher Akademischer Austauschdienst (DAAD, Grant No. A/01/19908). K. P. thanks the Development and Promotion of Science and Technology Talent Project (DPST), Thailand for financial support.

Appendix: Solution of Dirac equation for the effective potential

In this appendix we indicate the solutions to the Dirac equation with the effective potential $V_{\rm eff}(r) = S(r) + \gamma^0 V(r)$, with $r = |\boldsymbol{x}|$. The particular choice of scalar $S(r)$

and the time-like vector $V(r)$ parts are given by

$$S(r) = \frac{1-3\rho^2}{2\rho R} + \frac{\rho}{2R^3}\ r^2, \tag{60}$$

$$V(r) = \mathcal{E}_0 - \frac{1+3\rho^2}{2\rho R} + \frac{\rho}{2R^3}\ r^2. \tag{61}$$

The quark wave function $u_\alpha(\boldsymbol{x})$ in state α and eigenenergy $\mathcal{E}_\alpha$ with the specific choice of V_{eff} satisfies the Dirac equation

$$[-\mathrm{i}\gamma^0\boldsymbol{\gamma}\cdot\boldsymbol{\nabla} + \gamma^0 S(r) + V(r) - \mathcal{E}_\alpha]u_\alpha(\boldsymbol{x}) = 0. \tag{62}$$

The solution of the Dirac spinor $u_\alpha(\boldsymbol{x})$ to (62) can be written in the analytical form [17]:

$$u_\alpha(\boldsymbol{x}) \ = \ N_\alpha \begin{pmatrix} g_\alpha(r) \\ \mathrm{i}\boldsymbol{\sigma}\cdot\hat{\boldsymbol{r}} f_\alpha(r) \end{pmatrix} \mathcal{Y}_\alpha(\hat{\boldsymbol{r}})\chi_f\,\chi_c\,. \tag{63}$$

For the particular choice of potential the radial functions $g_\alpha(r)$ and $f_\alpha(r)$ satisfy the form

$$g_\alpha(r) = \left(\frac{r}{R_\alpha}\right)^l L_{n-1}^{l+1/2}\left(\frac{r^2}{R_\alpha^2}\right)\mathrm{e}^{-\frac{r^2}{2R_\alpha^2}}, \tag{64}$$

where for the $j = l + \frac{1}{2}$

$$f_\alpha(r) = \rho_\alpha\left(\frac{r}{R_\alpha}\right)^{l+1}\left[L_{n-1}^{l+3/2}\left(\frac{r^2}{R_\alpha^2}\right) + L_{n-2}^{l+3/2}\left(\frac{r^2}{R_\alpha^2}\right)\right]\mathrm{e}^{-\frac{r^2}{2R_\alpha^2}}, \tag{65}$$

and for $j = l - \frac{1}{2}$

$$f_\alpha(r) = -\rho_\alpha\left(\frac{r}{R_\alpha}\right)^{l-1}\left[\left(n+l-\frac{1}{2}\right)L_{n-1}^{l-1/2}\left(\frac{r^2}{R_\alpha^2}\right) + n\,L_n^{l-1/2}\left(\frac{r^2}{R_\alpha^2}\right)\right]\mathrm{e}^{-\frac{r^2}{2R_\alpha^2}}. \tag{66}$$

The label $\alpha = (nljm_j)$ characterizes the state with principle quantum number $n = 1, 2, 3, ...$, orbital angular momentum l, total angular momentum $j = l \pm \frac{1}{2}$ and projection m_j. Due to the quadratic nature of the potential the radial wave functions contain the associated Laguerre polynomials $L_n^k(x)$ with

$$L_n^k(x) = \sum_{m=0}^{n}(-1)^m\frac{(n+k)!}{(n-m)!(k+m)!m!}x^m. \tag{67}$$

The angular dependence, $\mathcal{Y}_\alpha(\hat{\boldsymbol{r}}) \equiv \mathcal{Y}_{ljm_j}(\hat{\boldsymbol{r}})$, is defined by

$$\mathcal{Y}_{ljm_j}(\hat{\boldsymbol{r}}) = \sum_{m_l,m_s}\left\langle l\,m_l\frac{1}{2}\,m_s\middle|j\,m_j\right\rangle Y_{lm_l}(\hat{\boldsymbol{r}})\chi_{\frac{1}{2}m_s} \tag{68}$$

where $Y_{lm_l}(\hat{\boldsymbol{r}})$ is the usual spherical harmonic. Flavor and color part of the Dirac spinor are represented by χ_f and χ_c, respectively.

The two coefficients R_α and ρ_α in the redial function of state α are of the form

$$R_\alpha = R(1 + \Delta\mathcal{E}_\alpha\rho R)^{-1/4}, \tag{69}$$

$$\rho_\alpha \ = \rho\left(\frac{R_\alpha}{R}\right)^3 \tag{70}$$

and are related to the Gaussian parameter ρ, R of equation (7). The quantity $\Delta\mathcal{E}_\alpha = \mathcal{E}_\alpha - \mathcal{E}_0$ is the excess of the energy of the quark state α with respect to the ground state. $\Delta\mathcal{E}_\alpha$ depends on the quantum number n and l and is related to the parameters ρ and R by

$$\left(\Delta\mathcal{E}_\alpha + \frac{3\rho}{R}\right)^2 \left(\Delta\mathcal{E}_\alpha + \frac{1}{\rho R}\right) = \frac{\rho}{R^3}(4n + 2l - 1)^2. \tag{71}$$

The normalization constant, which results in

$$N_\alpha = \left[2^{-2(n+l+1/2)}\pi^{1/2}R_\alpha^3 \frac{(2n+2l)!}{(n+l)!(n-l)!}\left\{1 + \rho_\alpha^2\left(2n + l - \frac{1}{2}\right)\right\}\right]^{-1/2}, \tag{72}$$

is obtained from the normalization condition

$$\int_0^\infty \mathrm{d}^3\boldsymbol{x}\, u_\alpha^\dagger(\boldsymbol{x}) u_\alpha(\boldsymbol{x}) = 1. \tag{73}$$

References

[1] Bernard V, Elouadrhiri L and Meißner Ulf-G 2002 *J. Phys. G: Nucl. Part. Phys.* **28** R1-R35
[2] Hagiwara K *et al* 2002 *Phys. Rev.* D **66** 010001
[3] Théberge S, Thomas A W and Miller G A 1980 *Phys. Rev.* D **22** 2838
Thomas A W, Théberge S and Miller G A 1981 *Phys. Rev.* D **24** 216
[4] Théberge S and Thomas A W 1983 *Nucl. Phys.* A **393** 252
[5] Thomas A W 1984 *Adv. Nucl. Phys.* **13** 1
[6] Chin S A 1982 *Nucl. Phys.* A **382** 355
[7] Gutsche Th 1978 *Ph.D.Thesis, Florida State University*
[8] Gutsche Th and Robson D 1989 *Phys. Lett.* B **229** 333
[9] Lyubovitskij V E, Gutsche Th and Faessler Amand 2001 *Phys. Rev.* C **64** 065203
[10] Lyubovitskij V E, Gutsche Th, Faessler Amand and Drukarev E G 2001 *Phys. Rev.* D **63** 054026
[11] Lyubovitskij V E, Gutsche Th, Faessler Amand and Vinh Mau R 2001 *Phys. Lett.* B **520** 204;
Lyubovitskij V E, Gutsche Th, Faessler Amand and Vinh Mau R 2002 *Phys. Rev.* C **65** 025202
[12] Lyubovitskij V E, Wang P, Gutsche Th and Faessler Amand 2002 *Phys. Rev.* C **66** 055204
[13] Cheedket S, Lyubovitskij V E, Gutsche Th, Faessler Amand, Pumsa-ard K and Yan Y 2002 *Preprint* hep-ph/0212347; accepted for publication in Eur Phys Jour A
[14] Pumsa-ard K, Lyubovitskij V E, Gutsche Th, Faessler Amand and Cheedket S 2003 *Phys. Rev.* C **68** 015205
[15] Inoue T, Lyubovitskij V E, Gutsche Th and Faessler Amand *Preprint* hep-ph/0311275; accepted for publication in Phys Rev C
[16] Takahashi T T, Matsufuru H, Nemoto Y and Suganuma H 2001 *Phys. Rev. Lett.* **86** 18
[17] Tegen R, Brockmann R and Weise W 1982 *Z. Phys.* A **307** 339
[18] Tegen R and Weise W 1983 *Z. Phys.* A **314** 357
[19] Oset E, Tegen R, Weise W 1984 *Nucl. Phys.* A **426** 456; [Erratum-ibid. 1986 **453** 751].
[20] Tegen R 1986 *Phys. Lett.* B **172** 153
[21] Tegen R 1989 *Phys. Rev. Lett.* **62** 1724
[22] Abbas A 1990 *J. Phys. G: Nucl. Part. Phys.* **16** L21
[23] Gell-Mann M and Lévy M 1960 *Nuovo Cimento* **16** 705
[24] Thomas A W 1981 *J. Phys. G: Nucl. Part. Phys.* **7** L283
[25] Morgan M A, Miller G A and Thomas A W 1986 *Phys. Rev.* D **33** 817
[26] Jennings B K and Maxwell O V 1984 *Nucl. Phys.* A **422** 589
[27] Gasser J, Sainio M E and Švarc A 1988 *Nucl. Phys.* B **307** 779
[28] Birse M C 1990 *Prog. Part. Nucl. Phys.* **25** 1
[29] Lu D H, Thomas A W and Williams A G 1998 *Phys. Rev.* C **57** 2628
[30] Ivanov M A, Locher M P and Lyubovitskij V E 1996 *Few Body Syst.* **21** 131
[31] Kambor J and Mojžiš M 1999 *JHEP* **9904** 031; Schweizer J 2000 *Ph.D.Thesis, University of Bern.*
[32] Becher T and Leutwyler H 2001 *JHEP* **0106** 017.
[33] Amaldi E *et al* 1970 *Nuovo Cimento* A **65** 377
[34] Amaldi E *et al* 1972 *Phys. Lett.* B **41** 216
[35] Bloom E D *et al* 1973 *Phys. Rev. Lett.* **30** 1186
[36] Brauel P *et al* 1973 *Phys. Lett.* B **45** 389
[37] Guerra A D *et al* 1975 *Nucl. Phys.* B **99** 253
[38] Esaulov A S, Pilipenko A M and Titov Y I 1978 *Nucl. Phys.* B **136** 511

Table 1. Contributions of the individual diagrams of Fig.2 to the axial charge g_A. Separate results for the inclusion of ground (GS) and excited states (ES) in the quark propagator are indicated.

	g_A
GS quark propagator	
3q-core	
LO	1.25
NLO	−0.06
Counterterm	−0.12
Exchange	0.23
Vertex correction	0.01
Self-energy	0.19
GS contribution	1.50
ES quark propagator	
NLO	−0.31
Counterterm	−0.25
Vertex correction	0.03
Self-energy	0.22
ES contribution	−0.31
Total(GS+ES)	1.19
Experiment[2]	1.267 ± 0.003

Table 2. Comparison of the axial mass and the axial radius between experimental values and the result from the PCQM.

	Model	Experiment
M_A (GeV)	0.78	1.069 ± 0.016[1]
$\langle r_A^2 \rangle^{1/2}$ (fm)	0.88	0.639 ± 0.010[1]

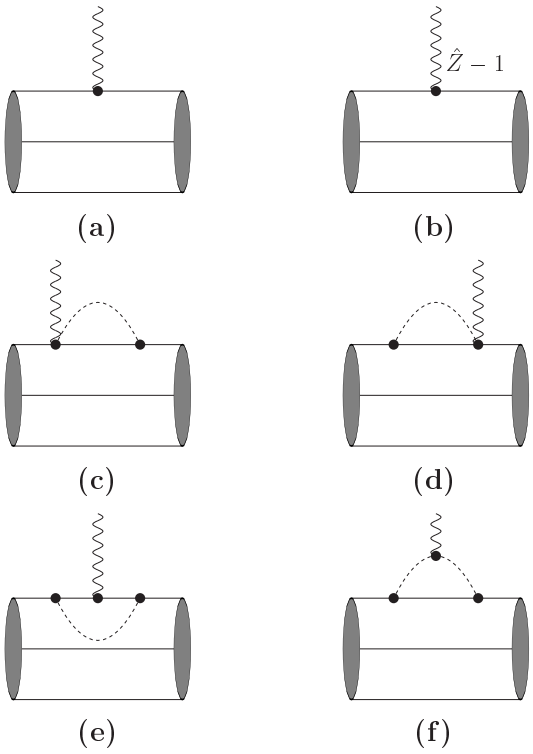

Figure 1. Diagrams contributing to the nucleon charge: triangle diagram (a), triangle counterterm diagram (b), self-energy diagrams (c) and (d), vertex correction diagram (e) and meson-cloud diagram (f).

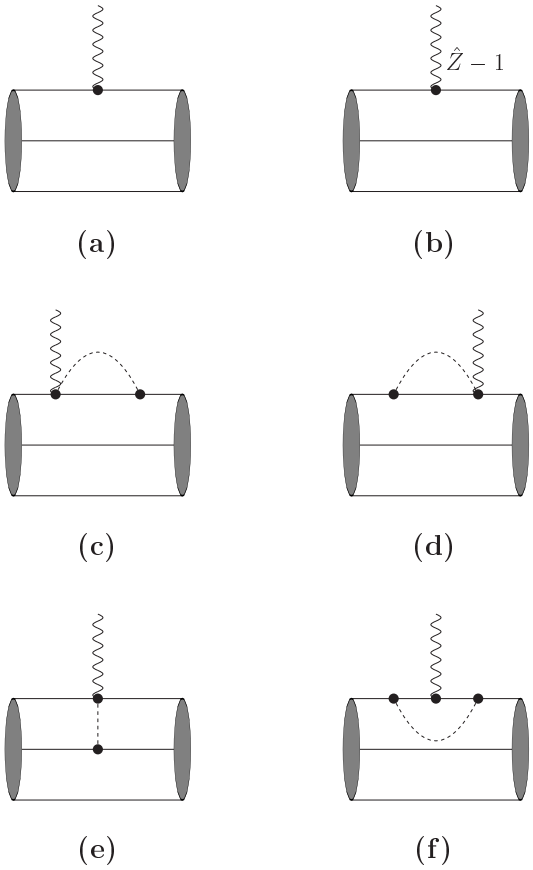

Figure 2. Diagrams contributing to the axial form factor of the nucleon : three-quark core (a), counterterm (b), self-energy (c and d), exchange (e) and vertex correction (f).

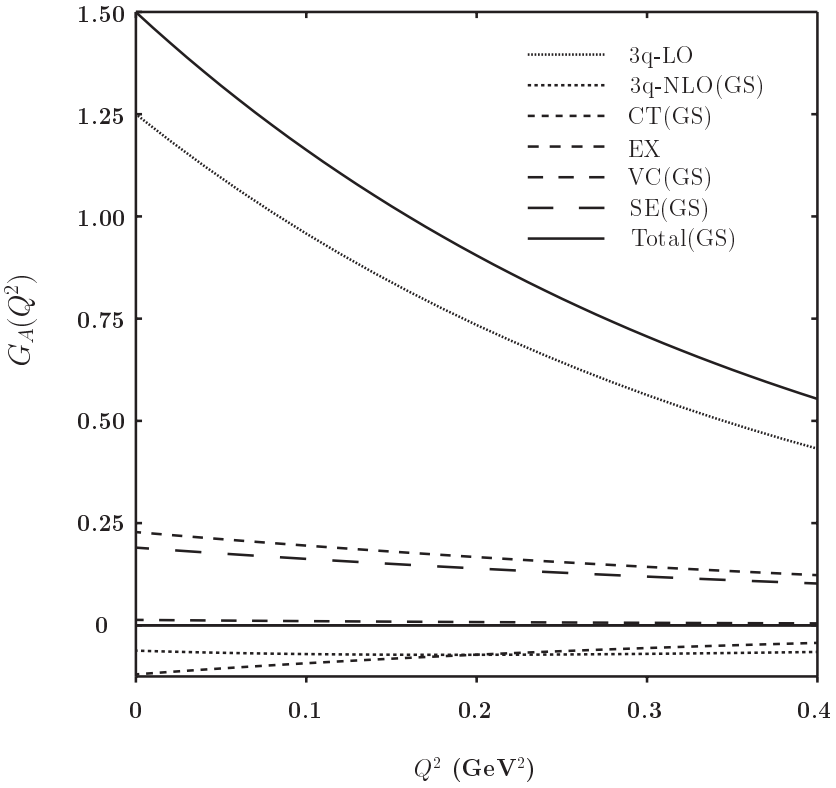

Figure 3. Model result for the axial form factor of the nucleon $G_A(Q^2)$. The coherent contributions of the different diagrams of Fig.2 are indicated when restricting to the ground state(GS) quark propagator.

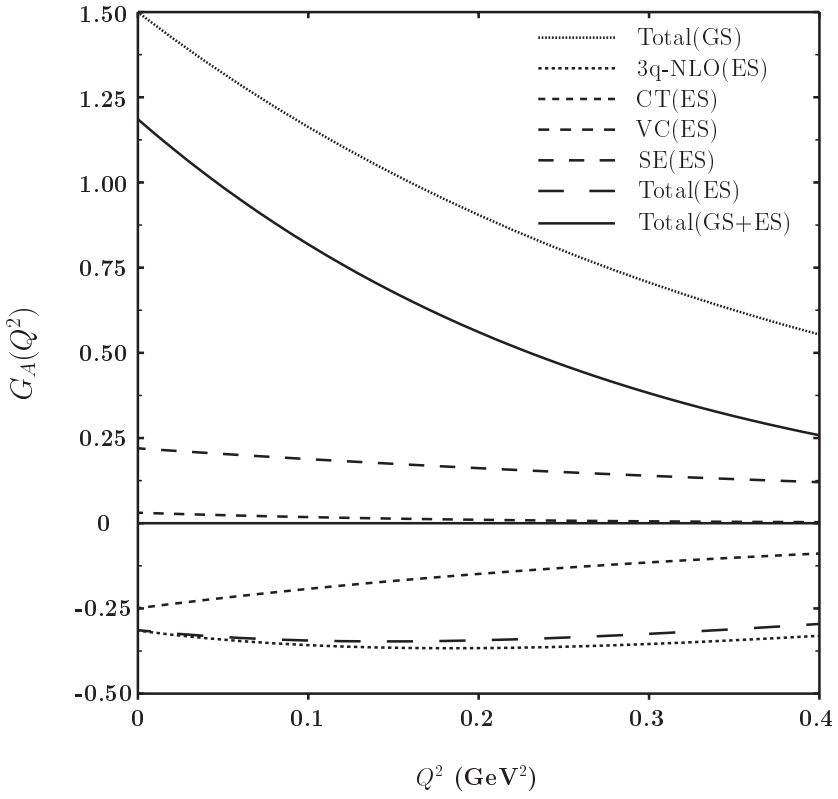

Figure 4. Model result for the axial form factor of the nucleon $G_A(Q^2)$ when excited states are included in the quark propagator. The full ground state result is contained in the curve labelled by Total(GS). Excited state (ES) contributions of the individual diagrams are indicated separately.

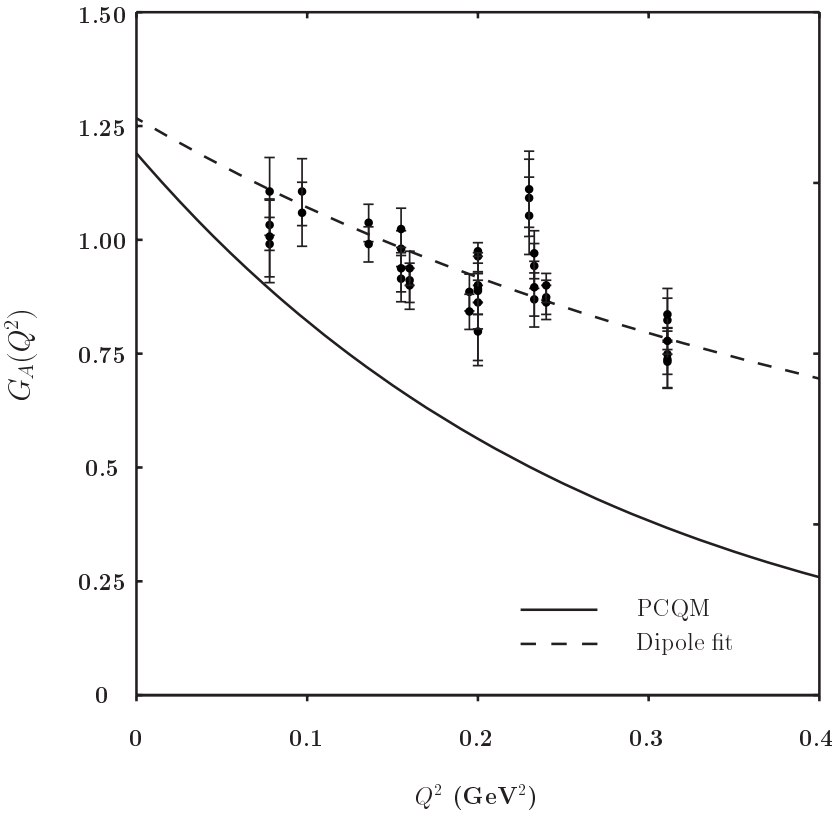

Figure 5. The axial form factor of the nucleon in the PCQM in comparison with a dipole fit (axial mass $M_A = 1.069$ GeV) and with experimental data. Data are taken from references [33]-[38].